ANNUAL REVIEWS

Annual Review of Analytical Chemistry

New Advances and Applications in Field-Flow Fractionation

Christine L. Plavchak,[1] William C. Smith,[1] Carmen R.M. Bria,[2] and S. Kim Ratanathanawongs Williams[1]

[1]Laboratory for Advanced Separation Technologies, Department of Chemistry, Colorado School of Mines, Golden, Colorado 80401, USA; email: krwillia@mines.edu

[2]Tolmar Inc., Fort Collins, Colorado 80524, USA

Annu. Rev. Anal. Chem. 2021. 14:257–79

First published as a Review in Advance on March 26, 2021

The *Annual Review of Analytical Chemistry* is online at anchem.annualreviews.org

https://doi.org/10.1146/annurev-anchem-091520-052742

Keywords

field-flow fractionation, separation, characterization, engineered nanomaterials, extracellular vesicles, polymer and protein assemblies, transformation and function

Abstract

Field-flow fractionation (FFF) is a family of techniques that was created especially for separating and characterizing macromolecules, nanoparticles, and micrometer-sized analytes. It is coming of age as new nanomaterials, polymers, composites, and biohybrids with remarkable properties are introduced and new analytical challenges arise due to synthesis heterogeneities and the motivation to correlate analyte properties with observed performance. Appreciation of the complexity of biological, pharmaceutical, and food systems and the need to monitor multiple components across many size scales have also contributed to FFF's growth. This review highlights recent advances in FFF capabilities, instrumentation, and applications that feature the unique characteristics of different FFF techniques in determining a variety of information, such as averages and distributions in size, composition, shape, architecture, and microstructure and in investigating transformations and function.

1. INTRODUCTION

MW: molecular weight or molar mass

ThFFF: thermal field-flow fractionation

SdFFF: centrifugal or sedimentation field-flow fractionation

FlFFF: flow field-flow fractionation

AF4: asymmetrical flow field-flow fractionation

D_T: thermal diffusion coefficient

NNP: naturally occurring nanoparticle

ENP: engineered nanoparticle

Nanometer- and larger-size analytes present formidable analytical challenges, as they are often heterogeneous mixtures with distributions in multiple physicochemical attributes or are part of complex mixtures (1–4). Adding to this complexity, some analytes are dynamic and undergo transformations that lead to changes in size, morphology, or surface chemistry and charge (5–7). For many of these cases, a separation technique and additional orthogonal methods are needed to obtain a more complete picture (8–10).

The use of external fields to achieve separations in an open channel lies at the heart of field-flow fractionation (FFF) techniques. One important feature is that it is a family of elution techniques and thus lends itself well to coupling with on-line detectors and collection of fractions containing purified or enriched subpopulations. The former creates a platform that incorporates orthogonal analyses of eluting enriched fractions within a single experiment. For example, the size of eluting nanoparticles (NPs) can be determined from retention time using FFF theory and by on-line multiangle and dynamic light scattering detectors or single-particle inductively coupled plasma mass spectrometry (spICP-MS). The FFF separation is important, as these detectors benefit from the increased monodispersity of the eluting sample fractions, and average values and distributions are determined. The ease of fraction collection post-FFF gives access to well-defined materials and biological species that are essential for investigating function. These and other attributes, such as FFF retention theories that are grounded in first principles, an open channel design that is highly conducive for probing fragile species and simultaneously monitoring species that span multiple orders of magnitude in size or molecular weight (MW), and flexibility in choice of carrier liquid, are some of the hallmarks expanded upon in later sections.

FFF is a group of distinctive techniques that utilize different types of fields, such as temperature gradient, centrifugal, and cross flow, giving rise to thermal (ThFFF), sedimentation (SdFFF or CF3), and flow FFF (FlFFF), respectively. **Figure 1** shows the general layout of an FFF channel and the types of fields that have been used thus far, along with the separation mechanism. The extent of retention in FFF depends on the magnitude of the interactions between the applied field and physicochemical properties of the analyte and the diffusion coefficient D of each analyte. Both factors lead to opposing transport that results in each analyte occupying a unique velocity streamline of the parabolic flow in the FFF channel. Each analyte is thus driven through the channel at different speeds and elutes at different times. An FFF technique may also have different variants. For example, FlFFF is commercially available in an asymmetrical (AF4) or a hollow fiber (HF5) channel format. Sample introduction and the requisite relaxation into unique equilibrium layers prior to the start of the separation can be implemented using different processes that include stop-flow (used in SdFFF), focusing flow (used in AF4), and frit inlet sample introduction with hydrodynamic relaxation. In addition to having different equipment, each FFF technique also has distinctive theories that relate retention time to analyte properties (2, 11). FlFFF separates on the basis of differences in D (or hydrodynamic diameter d_h), SdFFF separates according to differences in effective mass (or diameter and the difference in density between the analyte and the carrier liquid), and ThFFF differentiates according to analyte Soret coefficients (or the ratio of thermal diffusion coefficient D_T to D). For more details on retention theories and processes specific to each type of FFF field, refer to References 2, 4, and 11.

This review highlights the latest advances in FFF technology over the past decade and how FFF has contributed to the characterization of biological particles, naturally occurring NPs (NNPs) and engineered NPs (ENPs), and polymers, as well as to the understanding of transformations such as protein aggregation kinetics, NP degradation, and protein coronas. Practical considerations for FFF operation and challenges and opportunities of this technology are also discussed.

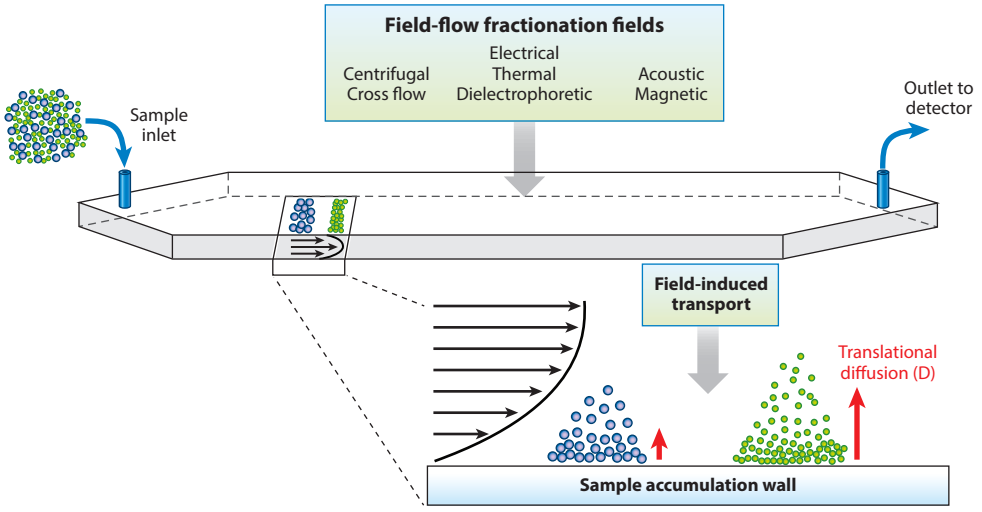

Figure 1

A simplified scheme of a field-flow fractionation (FFF) channel operating in normal mode. As analytes enter the channel, the applied field interacts with specific physicochemical properties of the analyte transporting it to the sample accumulation wall. The analyte's translational diffusion counteracts the field-induced transport, creating a steady state. This interplay leads to the formation of sample clouds whose average positions are in different flow velocity streamlines of the parabolic flow. In this schematic, the smaller particles diffuse faster and elute before the larger particles. FFF instruments with different externally applied fields, e.g., centrifugal, cross flow, electrical asymmetrical flow, and thermal, are available commercially. Electrical, acoustic, magnetic, and dielectrophoretic fields have also been successfully implemented.

2. APPLICATIONS

2.1. Cells and Subcellular Particles

The use of FFF in bioparticle characterization spans predictive diagnosis to biomarker discovery and therapeutic development. FFF's ability to separate and elute fractions of different sizes and mass components and to couple with multiple analytical methods has advanced understanding of biological content and function for cells, lipoproteins, extracellular vesicles (EVs), ribosomes, viruses, and virus-like particles (VLPs). Tumor formation, purification, and subassembly formation have also been examined, leading to insights into protein expression for diagnostics and vaccine development (12, 13). AF4 has been most utilized for these applications, with additional contributions from FlFFF, SdFFF, electrical FFF (ElFFF), and dielectrophoretic FFF (DEPFFF). The majority of FFF separations of bioparticles occur in the normal mode ($< \sim 1\ \mu m$), with cell separations occurring in the steric/hyperlayer mode ($> \sim 1\ \mu m$).

Label-free cell sorting is important for reducing costs of cell isolation in biological and clinical research. Current cell-sorting techniques rely heavily on cell-specific markers or chemical labels, which can lead to cell differentiation or apoptosis and potentially impact successive cultures. Hyperlayer mode SdFFF has shown promise as a tagless, noninvasive method for cell sorting (14). These advantages were demonstrated with human pluripotent stem cells and progenital cells (15). Tumor-initiating cells (TICs) are usually in low abundance (~1–5%) but are responsible for driving tumor growth and treatment resistance. SdFFF-sorted TICs were amplified to study tumor development, apoptosis, proliferation, vascularization, and protein expression (12). Cancer stem cells have been hypothesized to have variances in cell differentiation if grown on Classic

ElFFF: electrical field-flow fractionation

Medium compared to colorectal cancer–specific defined medium (16). This effect was confirmed with SdFFF. Additional efforts have focused on astrocyte subpopulations to help foster therapeutic approaches for improving neural stem cell function (17, 18). While SdFFF has been dominant in cell sorting, HF5's smaller volume is well suited for analyzing submicroliter sample volumes. HF5 columns are low cost and can be interchanged with the column on a high-performance liquid chromatography (HPLC) system (19, 20). The separation of tumor cells from blood cells and other cell types has been explored using DEPFFF (21, 22). The magnitude of the applied electric field can be constrained to localized regions of the channel, and targeted tumor cells can be levitated and ablated at higher microchannel positions. This configuration allows tumor cells to be removed while blood cells remain unharmed at the accumulation wall (21).

MALS: multiangle light scattering

DLS: dynamic light scattering

Analytical AF4 and semipreparative (SP)-AF4 have both contributed to advanced lipidomic characterization and aided in identifying lipoprotein markers for disease diagnostics (23–26). Analytical AF4 with offline liquid chromatography–tandem mass spectrometry is used for multiplexed lipoprotein analysis and provides an in-depth understanding of size-dependent compositional differences (23). Lipidomic analysis of SP-AF4 fractionated lipoproteins via nanoflow ultrahigh-performance liquid chromatography-electrospray ionization-tandem mass spectrometry (nUHPLC-ESI-MS/MS) introduced potential diagnostic methods for coronary artery disease, acute coronary syndrome (24), Alzheimer's disease (25), and postmenopausal osteoporosis (26). Lipoproteins from patients with these ailments had distinct differences in their lipidomes when compared to healthy control groups. Beyond evolving diagnostics and lipidomic analysis, a comparison of samples prepared by SP-AF4 and ultracentrifugation showed a 98% overlap in the high-density and low-density lipoprotein lipidome (27). Additionally, SP-AF4 isolated higher protein amounts per sample volume, was significantly faster (~1 h instead of multiple hours or days), and used buffers with lower ionic strengths, thereby reducing the likelihood of lipoprotein aggregation and damage or apolipoprotein dissociation. The ability to obtain quantitative measurements of lipoproteins with low starting volumes (100 μL) of serum postfractionation is significant compared to other methods.

Exosomes and EVs have come of interest owing to their potential as biomarkers and therapeutics and their role in cell signaling. The main challenge of characterizing these vesicles is the lack of knowledge of their biogenesis, composition, and biodistributions. FlFFF with offline nUHPLC-ESI-MS/MS analysis of pancreatic cancer exosomes helped determine disease status and elucidate size-dependent lipidomic differences (28). A landmark study used AF4-multiangle light scattering-dynamic light scattering (MALS-DLS) to isolate exosome subpopulations of melanoma cells (29, 30) (**Figure 2**). Postfractionation biochemical analyses revealed that each subpopulation had unique lipid, protein, and nucleic acid expression depending on the size, cell type, and vascular membrane structure. The in-depth protocol on exosome AF4 fractionation provided a framework for further developing EV separations. Beyond size and composition, the surface charge of EVs is also of interest and has been examined using cyclical electrical FFF (CyElFFF) (31).

AF4 and CyElFFF applications have expanded further into ribosomes (32), viruses (33), and VLPs (34). Recent work in this area has led to new questions about virology, how these materials are classified, and purification (35). AF4's low shear mitigates undesirable changes associated with traditional methods such as ultracentrifugation and sodium dodecyl sulfate-polyacrylamide gel electrophoresis (SDS-PAGE). Gentle purification using AF4 provided the unaltered samples necessary for identifying genome expression in the protein shell and lipid envelope. These two components are specific to host recognition of the virus and are vulnerable to biophysical and biochemical stresses (33). Enveloped bacteriophages, such as Φ6, are gaining interest because of their similarities to animal viruses. The use of anionic detergents can result in undesirable residual

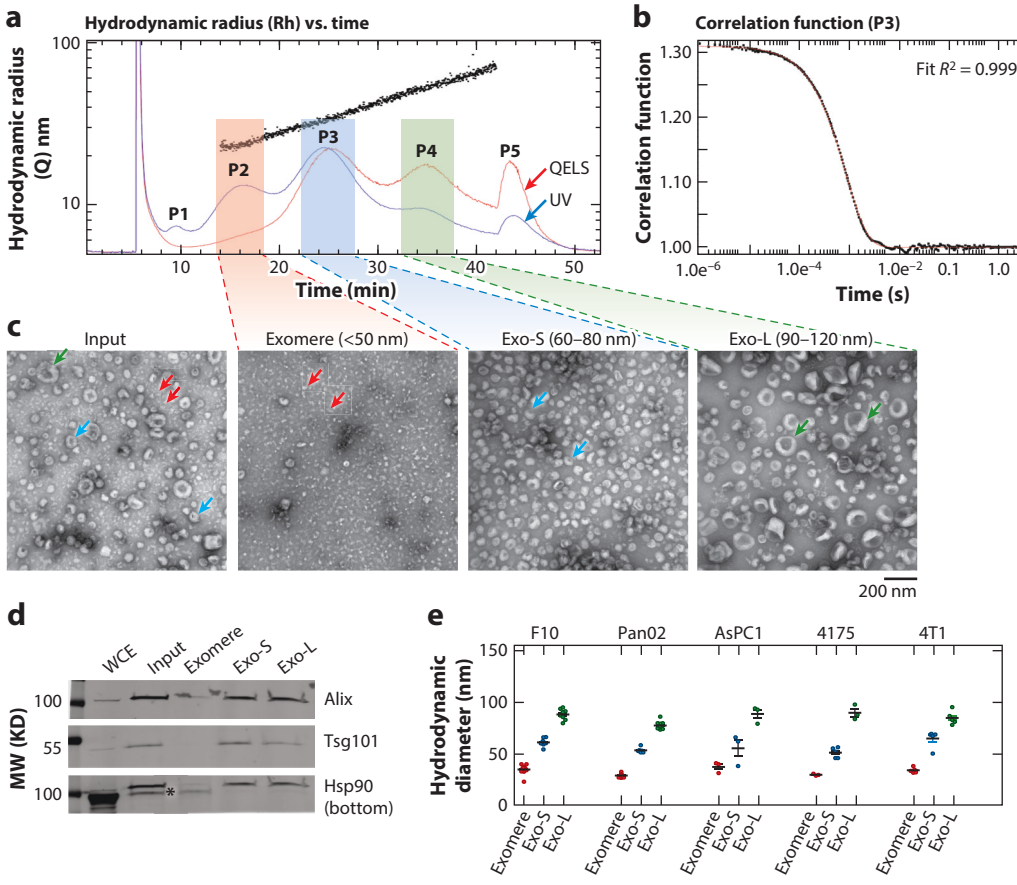

Figure 2

Asymmetrical flow field-flow fractionation (AF4) separation followed by orthogonal analyses have led to further understanding of extracellular vesicle (EV) heterogeneity. (*a*) AF4 separation of B10–F16 melanoma-derived EVs with ultraviolet spectroscopy (UV) and dynamic light scattering (DLS) detection shows five distinct peaks that correspond to unretained analytes (P1), a new class of vesicles termed exomeres (<50 nm, P2), small exosomes (60–80 nm, P3), large exosomes (90–120 nm, P4), and large aggregates (P5). The line above the fractograms corresponds to the hydrodynamic radius and confirms differences in size as a function of retention time. (*b*) A correlation function in QELS (quasielastic light scattering, also known as DLS) analysis corresponding to P3. (*c*) Transmission electron microscopy (TEM) images show vesicles in the stock solution prefractionation and the P2–P4 fractions collected after AF4 separation. (*d*) Western blot analyses confirmed the presence of exosomal proteins in whole-cell extract (WCE), exosome and exomere mixture (input), and three fractionated subpopulations. (*e*) Different cell lines F10, Pan02, AsPC1, 4175, and 4T1 show similar size distributions for all three populations of vesicles. Figure adapted with permission from Reference 29; copyright 2018 Springer Nature. Other abbreviation: MW, molecular weight.

and release of major proteins from the phage, a risk that has been mitigated using AF4. Beyond purification, AF4 has been used to study the disassembly of complex virions of phage Φ6. Through controlled dissociation treatments, biologically active subassemblies were identified based on their three distinct structural layers (36). CyElFFF-MALS-DLS has been utilized to determine electrophoretic mobilities of three Q beta bacteriophage VLPs containing different surface peptides (13). Understanding surface composition and partial separation of monomer and aggregated VLPs initiates further opportunities for CyElFFF use to characterize VLPs.

2.2. Engineered and Naturally Occurring Nanoparticles

ICP-MS: inductively coupled plasma mass spectrometry

The broad separation range and versatility of FFF provide a beneficial platform for the analysis of ENPs and NNPs, and most studies have employed AF4 and SdFFF (37). Typically, ENPs include metallic, metal-oxide, and polymeric NPs, while biopolymers, dissolved organic matter, and colloidal inorganic minerals are considered NNPs. Model ENP systems composed of polystyrene latex or SiO_2 are also commonly used to calibrate and evaluate FFF separations (38). Studies of ENPs and NNPs cover fate and transport, particle transformation, and interactions in complex media. Several comprehensive reviews cover ENPs and NNPs as synthesized (39) and in the environment (40, 41), consumer goods (42), and food (43).

As nanomaterials have become more common in consumer products, ENPs are inevitably released into the environment. ENPs and NNPs cannot be discriminated by size alone, and composition-sensitive detectors have proven to be important (43). AF4 coupled to ICP-optical emission spectrometry, ICP-MS, and spICP-MS are increasingly used combinations (44–46). These methods have enabled comprehensive size and composition characterization of ENPs, which is important for understanding their risk and fate in environmental matrices (47). Optimized extraction methods prior to analysis have shown that elemental ratios can be used to differentiate ENPs such as TiO_2 and CeO_2 from their NNP counterparts in soils (48). Other FFF techniques such as ThFFF or SdFFF can separate ENPs based on their size and surface or bulk composition to identify compositional heterogeneity. ThFFF separation and characterization of metallic and metal-oxide NPs as well as of multicomponent hybrids have exploited differences in NP thermal diffusion originating from surface and bulk composition differences (**Figure 3*a–d***) (49). SdFFF utilizes differences in effective mass for separating particles with differing bulk composition (50). Effective mass and particle volume from SdFFF and transmission electron microscopy (TEM) independently has also allowed comparative particle densities to be calculated (51).

When ENPs enter different chemical environments, they have the propensity to transform through aggregation, absorption, and/or dissolution mechanisms (52). Investigation of these transformations, especially below 10 nm, is important to understanding the fate, risk, and transport of ENPs in the environment. **Figure 3*e,f*** shows the AF4-UV-ICP-MS separation of *N*-vinyl-2-pyrrolidone-protected silver NPs (PVP-AgNPs) in the presence of tripeptide glutathione (GSH). The presence of GSH transformed the PVP-AgNP from a single larger NP population into a heterogeneous mixture composed of Ag^+, nanoclusters, and small NPs (5). Optimization of AF4 separation conditions enabled the identification of distinct NP and nanocluster subpopulations. This is the first study demonstrating AF4 isolation of ∼1-nm nanoclusters. Transformed particles exist in a spectrum that commonly goes unnoticed, particularly when they are introduced to environmental or biological systems (53). Multidetector approaches can identify and quantify species in this low size range and provide further insight into the size-specific risks associated with individual subpopulations of ions, metal-ligand complexes, nanoclusters, and NPs.

Carbon-based nanomaterials (e.g., fullerenes, carbon nanotubes, graphene) provide an additional challenge due to colloidal stability (54) and aggregation (55). High-resolution methods have been developed (56) to further understand aggregation mechanisms (6) and probe the interactions between ENPs and NNPs to study their fate in complex environmental media (57). Characterization of particle shape (e.g., structure, aspect ratio) has been of specific interest and highlights the benefits of AF4 (58–60). It is important to note that both the NP surfaces and carrier fluid composition can also strongly influence aggregation and interactions with the AF4 accumulation wall (61).

The potential environmental and health impacts of microplastics and nanoplastics are topics of intense interest (62). Both types of particles are highly challenging to separate and analyze

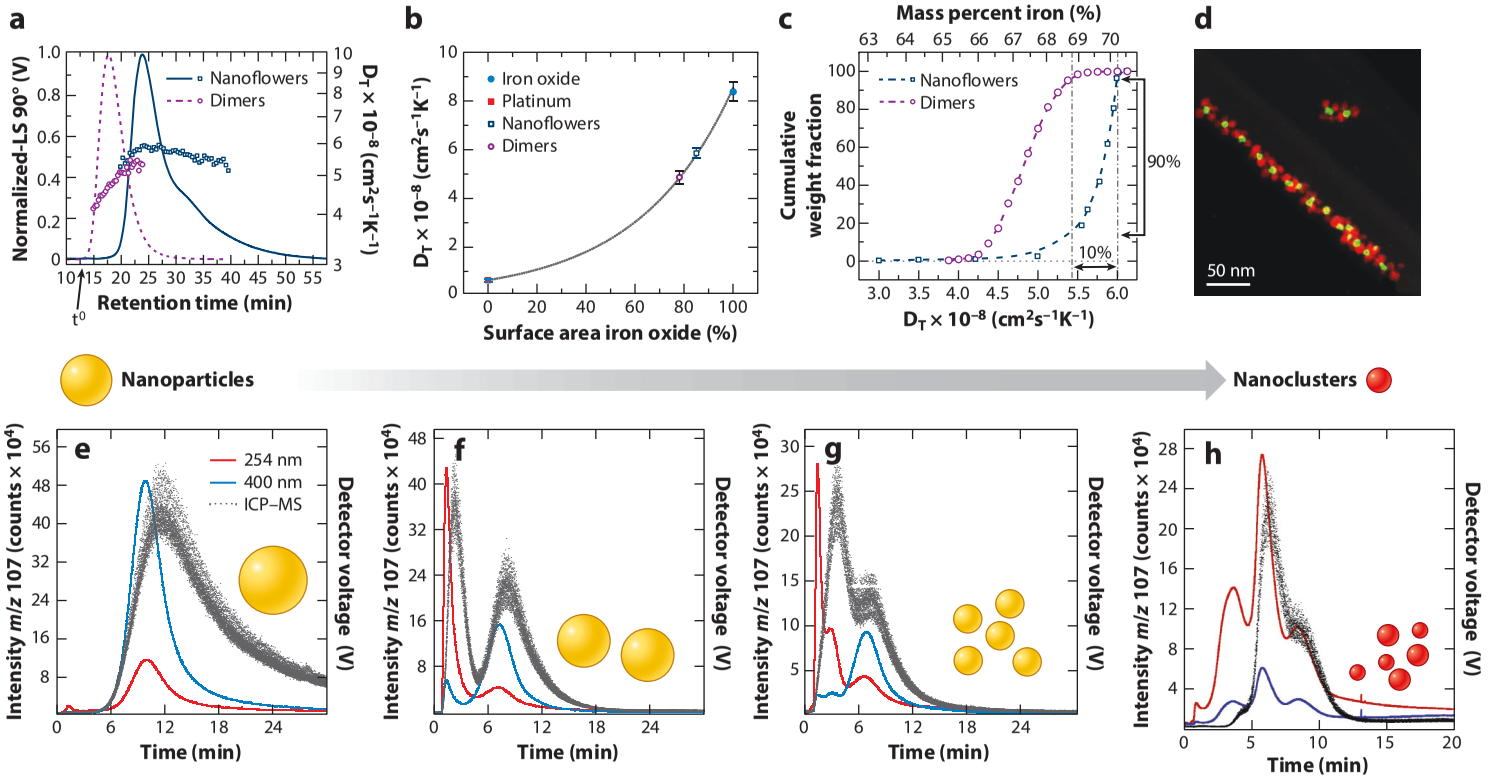

Figure 3

Capabilities of thermal field-flow fractionation (ThFFF) and asymmetrical flow field-flow fractionation (AF4) include composition distribution analysis of hybrid nanoparticles (NPs) and examination of NP-to-nanocluster (size) transformations, respectively. ThFFF composition sensitivity is reflected by the measured differences in thermal diffusion coefficient (D_T). (*a*) ThFFF fractograms of Pt-Fe_3O_4 hybrid NPs and variation in diffusion coefficient (D_T) as a function of retention time. These variations in D_T suggest compositional heterogeneity. (*b*) A thermal (D_T) calibration plot shows unique values for iron oxide particles and platinum cubes, dimers, and nanoflowers. (*c*) Cumulative weight fraction plots using D_T reveal that 90% of the nanoflower samples are compositionally monodisperse (mass % iron of 69–70%), while the dimer sample has more composition variation (90% of dimers have a mass % iron of 66–70%). Nanoflower composition was verified using (*d*) transmission electron microscopy-energy dispersive X-ray spectroscopy (TEM-EDS) elemental mapping high-angle annular dark field scanning (HAADF) of fractionated samples. Panels *a–d* adapted with permission from Reference 49; copyright 2018 American Chemical Society. Asymmetrical flow field-flow fractionation-ultraviolet spectroscopy-inductively coupled plasma mass spectrometry (AF4-UV-ICP-MS) can monitor changes to *N*-vinyl-2-pyrrolidone-protected silver NPs (PVP-AgNPs) (*e*) prior to the addition of excess glutathione (GSH), (*b*) 80 min after the addition of GSH, and (*c*) 4 days after the addition of GSH. Fractograms (*e–g*) show retention time changes that correlate with NP transformations to smaller-diameter species. (*h*) The AF4 method was further optimized to resolve three distinct populations of nanoclusters (1.8, 2.5, and 5.5 nm). Panels *e–h* adapted with permission from Reference 5; copyright 2013 American Chemical Society. Other abbreviation: LS, light scattering.

in an expedient manner because of their low numbers. AF4 in normal and steric modes demonstrated similar recoveries of nanoplastics and microplastics from aqueous environmental samples compared to analytical ultracentrifugation (3). AF4-MALS was used to detect nanoplastics in complex food matrices such as fish and helped optimize digestion protocols (63). Pyrolysis gas chromatography-MS and on-line Raman microspectroscopy have added important chemical characterization capabilities to the analysis of nanoplastics (3, 9).

The interaction of analytes with the sample accumulation wall and the subsequent effect on retention time have opened a new avenue of research. Analyte–wall interactions are generally governed by electrostatic and van der Waals forces, and the sum of dispersion forces can be described in terms of the Hamaker constant. Care is often taken to select a FlFFF membrane that minimizes these interactions based on the surface coating of the particles in question (64). Similar-sized nanomaterials have shown variation in AF4 retention time that can be correlated to these interactions via the Hamaker constants of the membrane and analyte (65). This link has enabled the development of an AF4 method for calculating an effective Hamaker constant for a given material in a variety of conditions and in various solvents (66). The ability to predict repulsive and attractive forces between particles and substrates could play an influential role in the development of colloidal assemblies and thin film technologies. Accordingly, this approach opens a new path to study interactions at nanomaterial surfaces and the role of surface functionalization.

2.3. Nanomaterials in Drug Delivery: Nanocarriers and Nanomedicines

Nanotherapeutics often take the form of polymer micelles and dendrimers, polymersomes, liposomes, stable emulsions, porous NPs, and other "nanocarriers." Many of these require a gentle separation technique owing to their delicate structures. This challenge makes AF4 uniquely suited for the analysis of biomedicines, and in-depth reviews of FFF for such analysis can be found elsewhere (67–70). The use of FFF has several benefits over batch methods such as DLS, including the quantification of populations undergoing aggregation or dissolution and examination of changes associated with drug delivery, storage, and release (71–73).

Polymeric nanocarriers, including micelles, dendrimers, and polymersomes, can be produced over a wide size range and with tunable chemical functionality. This flexibility enables them to carry both hydrophilic and hydrophobic therapeutics as well as control stability, lifetime, and therefore the release of drugs. The chemistry of the nanocarrier components and the composition of formulation buffer strongly impact the size, volume, and morphology of polymer micelles (74). Studies of block copolymer micelles via AF4-MALS-DLS determined the size, shape, and MW of such particles. In conjunction with hyphenated detection, changes in these properties with respect to the carrier fluid composition can be monitored and related to degradation and aggregation (75, 76). AF4-UV/vis-MALS has been used to study the impact of nanocarriers' size and colloidal stability on uptake, in vitro toxicity, and encapsulation of dyes for photodynamic therapy in block copolymer micelles (77). The release of therapeutics can be controlled via several mechanisms, including the response of nanocarriers to changes in the external chemical environment. The formulation and stability of polymersomes have been studied with respect to responses in variation of external pH and ionic strength (78). As observed in similar studies, a change in the pH environment may cause micelles to undergo morphological deformation and degradation (79). These studies highlight AF4's applicability to investigating formulation-based control of micelle morphology and how morphologies may exhibit differing degradation pathways and responses to changes in external environment. Similarly, porous inorganic and organic nanomaterials have shown promise for the loading and targeted delivery of proteins, dyes, and other therapeutics (80). Formulation of metal-organic frameworks for drug delivery has been studied by AF4-MALS, highlighting the

ability to monitor morphological changes, formation of aggregates, and the impact of drug loading on particle stability (81).

Nanostructured lipid carriers (82) and other emulsion-prepared therapeutics (83) for specific drug delivery have recently gained attention, with AF4 becoming a preferred method for particle characterization. Measurement of particle size distributions in medicinal products is especially important for understanding the biological effects of lipid-based nanotherapeutics (7). Understanding the aggregation, interaction, and assembly of liposomes with existing micelles and vesicles in biological matrices is necessary for a mechanistic understanding of the bioavailability and uptake of poorly water-soluble hydrophobic drugs (84). Although AF4 is a gentle separation technique compared to centrifugation and size exclusion chromatography (SEC), typical AF4 methodology involves a sample focusing step that has been noted to cause fusion of very small lipid particles into larger mixed micelles (72). To circumvent problems during sample focusing, researchers have investigated frit inlet versions of both FlFFF and AF4 and shown them to be good options (85). Specific uses of frit inlet FFF are discussed in Section 3. FlFFF techniques continue to meet the accelerating characterization needs of regulatory science (86) and help the further development of new nanotechnology-enabled pharmaceuticals and nanoformulations (87).

SEC: size exclusion chromatography

IgG: immunoglobulin G

dRI: differential refractive index

2.4. Assemblies and Complexes: Interactions of Polymers, Proteins, and Particles

Biologically derived drugs show promise for drug delivery and treatment. Assessing the interactions of these therapeutic candidates allows for a deeper understanding of factors controlling their efficacy. Aptamer-protein complexation was studied using a creative experimental design that exploited the physical characteristics of the AF4 channel. The cross flow field dictates that the channel wall must be semipermeable so analytes are retained but carrier liquid can permeate through. This feature enabled incubation of the aptamer-protein solutions during the focusing/relaxation step within the AF4 channel, followed immediately by separation and measurement of dissociation constants for aptamer-protein complexes (88). Determination of weak dissociation constants at a micromolar level were also shown for protein complexes, highlighting the potential for characterizing challenging binding systems (89).

Protein therapeutics show promise for disease treatment, but the formation of aggregates in formulations can reduce efficacy and potentially increase immunogenicity. AF4 provided the essential separation of anti-streptavidin immunoglobulin G (IgG) monomer from aggregates, whereas the MALS-differential refractive index (dRI) reported the MW of the eluting subpopulations. These data were fit to the Lumry–Eyring nucleated polymerization model, and kinetic analysis suggested that slow nucleation and aggregate condensation were the main pathways to the formation of nanometer and submicron aggregates (90). In addition, FFF's characteristic open channel permitted a comparative study of uncentrifuged and centrifuged heat-stressed anti-streptavidin IgG. (Centrifugation is commonly used as a sample preparation step to remove large-sized species that can clog chromatography columns.) AF4-MALS-dRI results suggested that the removal of large aggregates may influence aggregation kinetics. Polymeric protective agents that prevent aggregation during heat stress of IgG proteins were also studied using AF4 (91). Near the IgG unfolding temperature, polymer agents formed complexes with IgG to slow aggregate formation. Whole-blood separation by AF4 often requires extensive pretreatment owing to the large number of blood cells, platelets, and plasma present. However, a new AF4 method characterized protein therapeutics and their aggregates in whole blood (92). This is an exciting development that facilitates a better understanding of biotherapeutic behavior in complex biological media without disturbing aggregate species during sample preparation. Despite these successes, AF4 method development should consider the impact of sample injection, focusing, and separation on delicate

or transient aggregate populations (93). Additionally, the composition of the carrier fluid can impact protein retention due to protein–protein interactions and protein–membrane interactions (94).

Potential use of NP therapeutic delivery agents along with the prevalence of nanomaterials in the environment has raised questions about the fate of these materials in biologically relevant media (95). AF4 characterization of functionalized NPs (96), antibody-NP conjugates (97–99), functionalized carbon nanotubes (100), and protein-NP adsorption (101) has shown promise for understanding these complex systems. The protein corona formed on NP surfaces in biological media has also been studied. The nature of the protein corona–NP interactions and the relative dissociation rate of the protein corona were screened using AF4 and ultracentrifugation (102). The separation mechanism in AF4 allowed fast-dissociating proteins to be isolated from slow-dissociating proteins and the NPs. Differences in protein dissociation rates as NPs moved between different environments could have important implications for the protein corona. AF4 was compared to ultracentrifugation to show that loosely bound proteins (soft corona) could be preserved (103). In this study, polystyrene latex particles were incubated with human plasma and then separated using AF4 or ultracentrifugation. The identification of more human serum albumin and IgG proteins associated with the particles separated by AF4 confirmed the preservation of the soft protein corona compared to ultracentrifugation. Access to such NPs allowed further studies, concluding that only the hard protein corona impacted cell uptake behavior. Topological features of large biohybrid systems may play an important role in their applications but are challenging to analyze. Avidin and biotinylated glycodendrimer (GD-B) complexes were formed by varying the degree of biotinylation and the ligand–receptor stoichiometry and characterized by AF4-MALS-DLS-dRI (104). The apparent density, determined from the measured size and MW, and the MW dependence of the shape factor ($\rho = r_{rms}/r_h$), were examined to understand the scaling behavior of the avidin/GD-B_x structures. Conformation plots of ρ as a function of MW suggested the transformation from stiff rod-like structures to more branched microgels. This type of in-depth characterization is important for understanding the structure-function relationship of these large, complex, biohybrid systems.

Polymeric assemblies have potential use as delivery vectors for therapeutic treatments. Size and shape characterization for these assemblies is important for understanding their efficacy and function. Amphiphilic poly(ethyleneoxide-*b*-ε-caprolactone) (PEO-*b*-PCL) and poly(ethylene oxide-*b*-methylmethacrylate) block copolymer self-assemblies were characterized by AF4-MALS-DLS-dRI, and the results were compared to batch-mode light scattering, TEM, and atomic force microscopy to understand the morphologies of the formed polymersomes (79). Separation and identification of PEO-*b*-PCL micelles and vesicles by AF4 contributed to our understanding of the synergistic effects of polymersome morphology on photodynamic therapy cancer treatments (105). Comparison of AF4 and batch-mode DLS showed the poor suitability of the latter to accurately characterize complex mixtures of micelles and vesicles. The AF4-determined micelle and vesicle morphology distributions could be used to better understand the impact of polymersome morphology on the efficacy of photodynamic therapy during in vitro testing.

The analysis of shear-sensitive assemblies and complexes requires consideration of the FFF process, particularly the sample relaxation or focusing step where undesirable alteration of samples may occur. In such cases, frit inlet-FlFFF systems have proven to be a good alternative. Frit inlet-FlFFF and frit inlet-AF4 were shown to be suitable for characterizing shear-prone polyion complexes (PICs) (85). Batch-mode DLS measurements and conventional AF4 were unable to accurately characterize the complexes and dissociated the PICs, respectively. Frit inlet techniques not only preserved the self-assemblies but also identified changes in PIC compositions as a function of NaCl concentration. Frit inlet-AF4 has also improved characterization of

high-molecular-weight biopolymers such as glycogen and pullulan compared to conventional AF4 (106). The main drawback with frit inlet systems is lower separation resolution compared to conventional AF4.

The use of FFF to detect weakly bound biopolymer complexes, acquire topological information about biohybrid complexes, and determine the structures of micelles in complex mixtures represents state-of-the-art analyses. These types of studies are not as straightforward as those showing the well-documented capability of AF4 and light scattering to determine size and molar mass distributions. Despite significant method development and data analysis, this information content is difficult to achieve using other methods.

MWCO: molecular weight cutoff

3. DEVELOPMENTS IN INSTRUMENTATION AND ANALYSIS

Over the past decade, new applications have expanded the use of FFF, and advancing instrumentation and on-line detection capabilities have elevated FFF into emerging fields. AF4's widespread use has led to many developments in channel design and on-line instrumentation. Comparison of analytical AF4 channels with SP-AF4 has shown how channel design impacts overloading behavior and resolution (107). This work provides insights into SP-AF4 in both aqueous and organic solvents and highlights SP-AF4's potential for characterizing and collecting milligram quantities of different NPs.

At the analytical scale, microstructured membranes were developed and examined in efforts to increase retention, selectivity, and resolution. By hot-embossing a 30-kDa regenerated cellulose membrane with perpendicular grooves, an increase in retention of bovine serum albumin, γ- globulin, apoferritin, and thyroglobulin was achieved (108). Further optimization with lower molecular weight cutoff (MWCO) membranes, membrane fabrication processes, and COMSOL modeling helped increase the selectivity and resolution for smaller MW analytes. This initial structured membrane work led to a potentially high-throughput, two-dimensional (2D) fractionation for proteins and NP mixtures using frit inlet-AF4 (109).

Long-standing analysis centered around metal NPs and aquatic samples has led to developments involving the coupling of ICP-MS with AF4. Owing to MWCO limitations for AF4 membranes, an interface was recently developed to direct cross flow fluid from AF4 into the ICP-MS (110). Monitoring the dissolved analytes in the cross flow and particulates in the channel flow of AF4 with ICP-MS increased the efficiency of analysis. The abundance of particles between 0.3 and 1 kDa in natural waters has led to the use of low (∼300-Da) MWCO membranes that necessitated channel modifications to handle higher channel pressures (111). Lower-MWCO membranes used for dissolved organic matter could open a new realm of analysis to AF4 that has often been dominated by SEC, including oligomeric polymer species in a variety of solvents, and better facilitate the monitoring of degradation and dissolution of ENPs by ICP-MS. Comparison of spICP-MS and AF4-ICP-MS in regard to size resolution and multiform metal analysis has shown AF4-ICP-MS to have better size resolution, providing an understanding of NP complexation and aggregation (47).

Beyond ICP-MS, other novel detection schemes have recently been coupled to AF4 channels, including a liquid waveguide capillary cell (LWCC) (10), optical-trap-based Raman flow cell (9), and a γ-ray detector (112). A longer optical path length for the capillary cell coupling of LWCC to AF4 has provided enhanced sensitivity of AgNPs down to the part-per-billion level without any preconcentration steps. The development of optical-trap flow cells for Raman microspectroscopy and coupling to AF4 and CF3 (or SdFFF) are major breakthroughs in on-line chemical analysis of <1-μm particles. This has allowed the identification of polystyrene latex

g″: Soret contraction factor

and polymethylmethacrylate particles (9) and overcomes the size and compositional limitations observed in traditional Raman spectroscopy. Coupling a γ-ray detector to an AF4 channel serves as a stepping stone in the analysis of theragnostic particles used in radiation and alpha therapy. This powerful tool consolidates analysis time by monitoring liposome sizes and retention of radioactive metal within the lipid vesicles. This allows AF4 to be used in tracking the dissolution, release, and retention of radioactive components in vesicles after they are incubated in biologically relevant media such as human blood serum.

The rise in bioparticle analysis has led to an increased interest in particle counting. Traditional batch methods such as flow cytometry, particle tracking analysis, and resistive-pulse sensing are often hindered by polydisperse analytes, instrument sensitivity, and operator error (113, 114). More recently, NP tracking analysis has been successfully coupled to AF4, demonstrating its potential for on-line particle counting (8). Particle counting with AF4-MALS is also gaining attention, yet little work has been done in this area thus far (115, 116).

Recently updated designs have been implemented to analyze particles spanning the 1–10 μm size range utilizing an acoustic force field for a separation based on particle size and density and physical properties of the solvent. Unlike previous acoustic FFF systems where the acoustic radiation forces provide lift to sedimenting particles (in opposition to the gravitational field), this system was designed to suppress diffusive and lift forces by accelerating sedimentation velocity (117). This novel approach minimized sample relaxation time, thus enabling faster analyses over a wider separation range and with enhanced resolution over traditional gravitational FFF. These advancements make acoustic FFF a promising technique for high-throughput screening of micron-sized particles.

Surface charge is important for understanding macromolecular and particle interactions. This capability was realized by the introduction of electrical asymmetrical flow FFF (EAF4), which can separate particles and macromolecules by size and charge while providing orthogonal determination of electrophoretic mobilities and zeta potentials (118). EAF4 is an improvement over phase analysis light scattering for polydisperse systems, as it can measure the distribution of surface charges as a function of size. Polystyrene latex beads and proteins showed increased resolution and fractionating power over FlFFF techniques.

The past five years have seen advancements in polymer analysis using ThFFF (119). The increased use of on-line MALS-dRI detectors has revealed issues with the analysis of high MW and complex polymers by size exclusion chromatography (120–123). A new approach to determining the degree of branching and distributions of architecture exploited the Soret coefficient measured by ThFFF. Similar to other contraction factors obtained by light scattering and viscometry, the Soret contraction factor g″ from ThFFF could provide insight into the degree of branching and distributions of architecture (124). This work deconvoluted subtleties in architecture for aromatic-aliphatic polyesters (**Figure 4*a***). Similar work followed with examining chain-walking polyethylene polymers but with an alternative approach to determine g″ (125). Both studies showed a significant influence of solvent selection on polymer topology when calculating the thermal diffusion coefficient DT for the polymer system. In conjunction with g″, 2D separations conducted with both ThFFF and SEC have provided detailed size and compositional information for polystyrene-poly(methyl methacrylate) (126). The sensitivity of ThFFF separations to polymer microstructure has also been demonstrated (127) (**Figure 4*b***), and the effect of microstructure on stereocomplexation of polymers during micelle formation and annealing was investigated in subsequent ThFFF studies (128). The ability of ThFFF to analyze both the polymeric precursors and their self-assemblies by size, composition, and architecture/morphology has implications for the characterization of polymer micelles, polyplexes, and polymer aggregate systems being designed for numerous industrial applications (129).

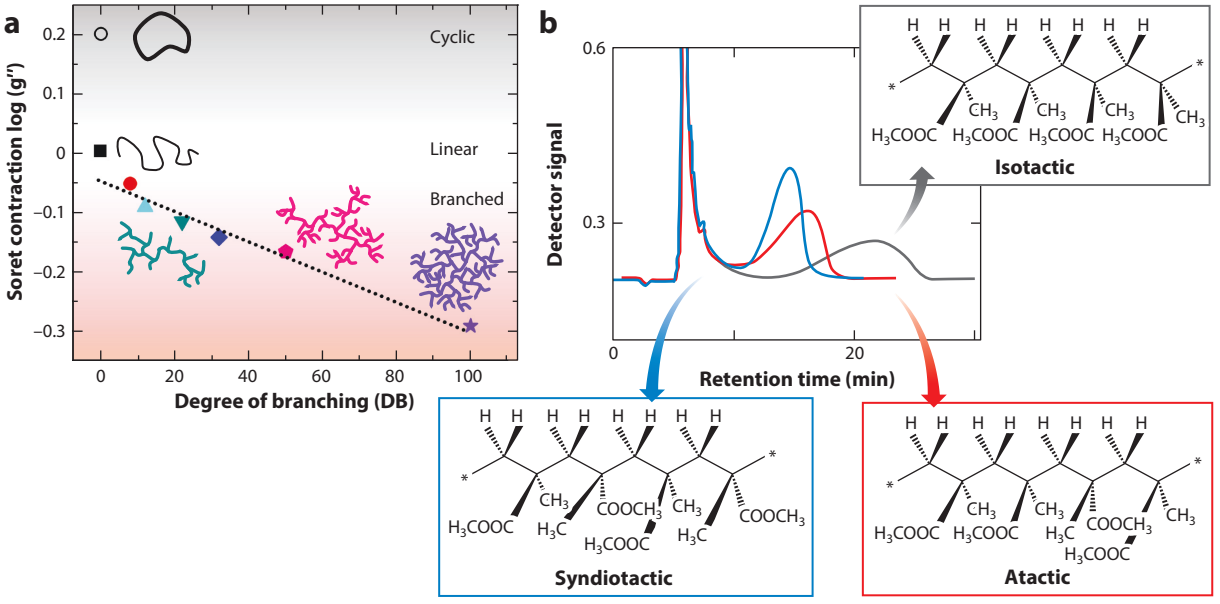

Figure 4

A new approach to polymer architecture and tacticity analysis uses parameters measured by thermal field-flow fractionation (ThFFF). (*a*) Degree of branching (DB) distributions are determined for a series of aromatic-aliphatic polyesters with varying DB. Soret coefficients calculated from measured retention times of branched and linear polymers of the same molecular weight (MW) are ratioed to yield a Soret contraction factor g″. An increase in DB from linear to pseudodendritic polyesters correlated with a decrease in the Soret contraction factor (g″) and yielded an architecture calibration plot. Low-MW species with positive g″ values were collected after elution from ThFFF, examined by matrix-assisted laser desorption ionization-time-of-flight mass spectrometry (MALDI-TOF MS) and found to be cyclic polyester species. Panel adapted with permission from Reference 124; copyright 2019 American Chemical Society. (*b*) Three poly(methyl methacrylate) samples of similar MW and different tacticity show varying retention time (t_r) in acetonitrile. Owing to the similar translational diffusion coefficients, the difference in t_r during ThFFF fractionation is suggested to be driven by the polymer microstructure. Rigidity in the isotactic sample has been observed to increase thermal diffusion coefficient (D_T) compared to syndiotactic and atactic samples. Panel adapted with permission from Reference 127; copyright 2015 American Chemical Society.

4. PRACTICAL CONSIDERATIONS

Proper selection of FFF technique, separation conditions, carrier liquid, sample accumulation wall, and detection method is central to obtaining meaningful results. Most recent work addressing these practical considerations focuses on AF4 but can be applied to all FFF techniques. The wide range of AF4 applications has led to many sample specific methods. The creation of a standard method development workflow for NP characterization by AF4 provides guidance for novice and expert users (130), and the standardization of AF4 and CF3 methods has been established in an International Organization for Standardization method (131). A critical overview of FlFFF also provides users with the fundamental theory and relevant factors that impact analysis (132). The overview offers practical recommendations for common problems, a discussion of the strong and weak points of FlFFF, and recommendations for good method development and reporting practices. Other recent publications present excellent practical and theoretical discussions (133–139). Some additional impactful and practical examples are reviewed below.

Carrier fluid ionic strength is important for controlling electrostatic interactions between the FlFFF membrane and analytes. Ions can accumulate near the semipermeable membrane and reduce the Debye length, leading to increased particle–membrane interactions and thus sample loss (140). Higher-charge-state anions accumulate more than lower-charge-state anions, highlighting

the need for careful carrier fluid composition selection. Sample composition is also important for selecting FFF conditions because the sample loss mechanism can vary significantly between samples. Gold NPs (AuNPs) stabilized by citrate or polyethylene glycol (PEG) chains with varying MW were shown to have different sample loss mechanisms during AF4 analysis (141). The relatively weakly bound citrate compared to the covalently bonded PEG chains resulted in more sample loss for citrate stabilized AuNPs than PEG-stabilized particles. Most of the sample loss for citrate AuNPs was due to the polyetheretherketone tubing rather than the AF4 membrane. At low ionic strengths, electrostatic repulsion between particles and the membrane resulted in lower sample loss; higher ionic strengths led to increased sample loss due to bridging interactions between the PEG chains and the membrane. Additionally, membrane "hot spots" of AuNP adsorption were observed, which is a reminder that membrane heterogeneity still remains a weak point for FlFFF (142).

The FFF separation mechanism under ideal conditions is well established. Recent work has strengthened the understanding of how nonidealities influence separation. For instance, the impact of cooperative diffusion of silica NPs was demonstrated during AF4 analysis (143). Faster-diffusing 50-nm particles were shown to significantly increase the diffusion of the slower-diffusing 100-nm particles, resulting in poor size resolution. Cooperative diffusion effects could be eliminated by reducing both sample load and Debye length by adding sodium dodecyl sulfate. Theoretical and experimental studies of the impact of secondary relaxation during flow programming as well as improvements to determine the channel thickness parameter have also been reported (133, 134). Recent theoretical work that calculated the nonparabolicity correction of laminar flow profiles in 59 solvents will continue to improve accuracy of the retention parameter determined for ThFFF (144).

Coupling light scattering detectors with FFF separations has become standard practice and enables fast, accurate, and in-depth characterization. The shape factor (r_{rms}/r_h) obtained from on-line MALS and DLS measurements permitted determination of particle shape. However, the accuracy of these measurements is key to ensuring proper determination of the shape factor. Channel or detector flow rate has been shown to impact DLS measurements owing to additional translational motion along with Brownian motion and analyte deformation (145). Increasing flow rate from 0.2 to 1 mL/min had a significant impact on DLS accuracy for particles $\geq$100 nm, with higher flow rates and larger particles contributing to the largest errors. Manufacturers have recognized erroneous DLS measurements, and advancements have been made to improve accuracy. Extension of the Rayleigh–Ganz light scattering theory to more complex NP structures, such as ellipsoids, rods, and tubes, facilitated the characterization of complex shapes (146). For instance, determining rod length distributions using a rod model can be done directly using FFF-MALS data when the rod diameter is known. The parallel development and understanding of FFF separations and MALS analysis for nonspherical particles offer an exciting path forward.

In addition to NP size and shape characterization, FFF-MALS is now often used for determining absolute MW and r_{rms} distributions, especially for high-MW ($>10^6$ g/mol) polymers and proteins. Coelution effects observed as a downturn or upturn in the MW determined by on-line MALS-dRI measurements across AF4 fractograms have been encountered in complex sample mixtures (147). Downturns may be observed in light scattering data, often thought of as an artifact, but they are caused by compact glycogen having a smaller size and similar MW to pullulan. Upturns may also be observed showing coelution of a mixture with overlapping size distributions but different MW distribution. While coelution can be observed for two or more distinct polymers, this phenomenon may be indicative of a sample mixture of a single-polymer composition containing both linear and branched chains, complexes, or aggregates. Furthermore, samples with broad size

distributions that span ~1 μm will cross the steric transition and result in reverse elution order of the largest components (148). In this case, coelution causes poor Zimm plot fits that bias the r_{rms} determination toward larger sizes. Separation conditions can be adjusted to reduce or eliminate this coelution, but samples must often be filtered or centrifuged to remove the large components. The expansion of FFF techniques to new users and to address new challenges continues to push current instrument capabilities.

5. CONCLUSION AND FUTURE TRENDS

FFF continues to be used for separating and characterizing macromolecules, NPs, colloids, and micrometer-sized particles with the goal of determining average size, MW, and density as well as distributions representative of heterogeneity in these various primary properties. In the last decade, FFF techniques coupled with orthogonal analyses have broadened the scope of investigative studies of increasingly complex systems where questions about nanomaterial transformations and bioparticle functions can start to be answered. In doing so, FFF has helped tie different fields together. Moving forward, FFF will likely play an important role in new fields such as nanoplastics and their environmental and biological impacts, design and function of smart materials, and classification and purpose of extracellular vesicles. Despite the observed growth, FFF is not yet a standard technique in analytical laboratories. Challenges and opportunities are plentiful and include improving the robustness of membranes for AF4 and methods to obtain a reproducible membrane surface from day to day; obtaining a better understanding of thermal diffusion and other secrets it may hold with respect to unlocking new characterization capabilities; standardizing protocols for specific high-impact applications; decreasing instrumental band broadening; further flattening the learning curve for new users through simulations and machine learning; and developing sensitive on-line composition detectors and capabilities for nonspherical analytes.

DISCLOSURE STATEMENT

The authors are not aware of any affiliations, memberships, funding, or financial holdings that might be perceived as affecting the objectivity of this review.

ACKNOWLEDGMENTS

This work was supported by a grant from the US National Science Foundation (CHE-1808805).

LITERATURE CITED

1. Johnston LJ, Gonzalez-Rojano N, Wilkinson KJ, Xing B. 2020. Key challenges for evaluation of the safety of engineered nanomaterials. *NanoImpact* 18:100219–29
2. Williams SKR, Runyon JR, Ashames AA. 2011. Field-flow fractionation: addressing the nano challenge. *Anal. Chem.* 83(3):634–42
3. Mintenig SM, Bäuerlein PS, Koelmans AA, Dekker SC, van Wezel AP. 2018. Closing the gap between small and smaller: towards a framework to analyse nano- and microplastics in aqueous environmental samples. *Environ. Sci. Nano* 5(7):1640–49
4. Contado C. 2017. Field flow fractionation techniques to explore the "nano-world." *Anal. Bioanal. Chem.* 409(10):2501–18
5. Pettibone JM, Gigault J, Hackley VA. 2013. Discriminating the states of matter in metallic nanoparticle transformations: What are we missing? *ACS Nano* 7:2491–99

6. Gigault J, Grassl B. 2017. Improving the understanding of fullerene (nC_{60}) aggregate structures: fractal dimension characterization by static light scattering coupled to asymmetrical flow field flow fractionation. *J. Colloid Interface Sci.* 502:193–200
7. Caputo F, Arnould A, Bacia M, Ling WL, Rustique E, et al. 2019. Measuring particle size distribution by asymmetric flow field flow fractionation: a powerful method for preclinical characterization of lipid-based nanoparticles. *Mol. Pharm.* 16:756–67
8. Adkins GB, Sun E, Coreas R, Zhong W. 2020. Asymmetrical flow field flow fractionation coupled to nanoparticle tracking analysis for rapid online characterization of nanomaterials. *Anal. Chem.* 92:7071–78
9. Schwaferts C, Sogne V, Welz R, Meier F, Klein T, et al. 2020. Nanoplastic analysis by on-line coupling of Raman microscopy and field-flow fractionation enabled by optical tweezers. *Anal. Chem.* 92:5813–20
10. Kim ST, Cho H-R, Jung EC, Cha W, Baik M-H, Lee S. 2017. Asymmetrical flow field-flow fractionation coupled with a liquid waveguide capillary cell for monitoring natural colloids in groundwater. *Appl. Geochem.* 87:102–7
11. Schimpf ME, Caldwell KD, Giddings JC. 2000. *Field Flow Fractionation Handbook*. New York: Wiley
12. Mélin C, Perraud A, Christou N, Bibes R, Cardot P, et al. 2017. New ex-ovo colorectal-cancer models from different SdFFF-sorted tumor-initiating cells. *Anal. Bioanal. Chem.* 407:8433–43
13. Shiri F, Petersen KE, Romanov V, Zou Q, Gale BK. 2020. Characterization and differential retention of Q beta bacteriophage virus-like particles using cyclical electrical field-flow fractionation and asymmetrical flow field-flow fractionation. *Anal. Bioanal. Chem.* 412:1563–72
14. Naves T, Battu S, Jauberteau M-O, Cardot PJP, Ratinaud M-H, Verdier M. 2012. Autophagic subpopulation sorting by sedimentation field-flow fractionation. *Anal. Chem.* 84:8748–55
15. Faye P-A, Vedrenne N, De La Cruz-Morcillo MA, Barrot C-C, Richard L, et al. 2016. New method for sorting endothelial and neural progenitors from human induced pluripotent stem cells by sedimentation field-flow fractionation. *Anal. Chem.* 88:6696–702
16. Mélin C, Perraud A, du Puch CBM, Loum E, Giraud S, et al. 2014. Sedimentation field-flow fractionation monitoring of *in vitro* enrichment in cancer stem cells by specific serum-free culture medium. *J. Chromatogr. B.* 963:40–46
17. Vedrenne N, Sarrazy V, Battu S, Bordeau N, Richard L, et al. 2016. Neural stem cell properties of an astrocyte subpopulation sorted by sedimentation field-flow fractionation. *Rejuvenation Res.* 19(5):362–72
18. Sarrazy V, Vedrenne N, Bordeau N, Billet F, Cardot P, et al. 2013. Fast astrocyte isolation by sedimentation field flow fractionation. *J. Chromatogr. A* 1289:88–93
19. Mélin C, Lacroix A, Lalloué F, Pothier A, Zhang LY, et al. 2013. Improved sedimentation field-flow fractionation separation channel for concentrated cellular elution. *J. Chromatogr. A* 1302:118–24
20. Ibrahim T, Battu S, Cook-Moreau J, Cardot P. 2012. Instrumentation of hollow fiber flow field flow fractionation for selective cell elution. *J. Chromatogr. B* 901:59–66
21. Kinio S, Mills JK. 2017. Localized electroporation with dielectrophoretic field flow fractionation: toward removal of circulating tumour cells from human blood. *IEEE Trans. Nanobiosci.* 16(8):802–9
22. Shamloo A, Kamali A. 2017. Numerical analysis of a dielectrophoresis field-flow fractionation device for the separation of multiple cell types. *J. Sep. Sci.* 40:4067–75
23. Kuklenyik Z, Jones JI, Gardner MS, Schieltz DM, Parks BA, et al. 2018. Core lipid, surface lipid and apolipoprotein composition analysis of lipoprotein particles as a function of particle size in one workflow integrating asymmetric flow field-flow fractionation and liquid chromatography-tandem mass spectrometry. *PLOS ONE* 13:e0194797
24. Lee JH, Yang JS, Lee S-H, Moon MH. 2018. Analysis of lipoprotein-specific lipids in patients with acute coronary syndrome by asymmetrical flow field-flow fractionation and nanoflow liquid chromatography-tandem mass spectrometry. *J. Chromatogr. B* 1099:56–63
25. Kim SH, Yang JS, Lee JC, Lee J-Y, Lee J-Y, et al. 2018. Lipidomic alterations in lipoproteins of patients with mild cognitive impairment and Alzheimer's disease by asymmetrical flow field-flow fractionation and nanoflow ultrahigh performance liquid chromatography-tandem mass spectrometry. *J. Chromatogr. A* 1568:91–100

26. Lee KG, Lee GB, Yang JS, Moon MH. 2020. Perturbations of lipids and oxidized phospholipids in lipoproteins of patients with postmenopausal osteoporosis evaluated by asymmetrical flow field-flow fractionation and nanoflow UHPLC–ESI–MS/MS. *Antioxidants* 9:46
27. Bria CRM, Afshinnia F, Skelly PW, Rajendiran TM, Kayampilly P, et al. 2019. Asymmetrical flow field-flow fractionation for improved characterization of human plasma lipoproteins. *Anal. Bioanal. Chem.* 411:777–86
28. Yang JS, Lee JC, Byeon SK, Rha KH, Moon MH. 2017. Size dependent lipidomic analysis of urinary exosomes from patients with prostate cancer by flow field-flow fractionation and nanoflow liquid chromatography-tandem mass spectrometry. *Anal. Chem.* 89:2488–96
29. Zhang H, Freitas D, Kim HS, Fabijanic K, Li Z, et al. 2018. Identification of distinct nanoparticles and subsets of extracellular vesicles by asymmetric flow field-flow fractionation. *Nat. Cell Biol.* 20(3):332–43
30. Zhang H, Lyden D. 2019. Asymmetric-flow field-flow fractionation technology for exomere and small extracellular vesicle separation and characterization. *Nat. Protoc.* 14(4):1027–53
31. Petersen KE, Shiri F, White T, Bardi GT, Sant H, et al. 2018. Exosome isolation: cyclical electrical field flow fractionation in low-ionic-strength fluids. *Anal. Chem.* 90(21):12783–90
32. Eskelin K, Varjosalo M, Ravantti J, Mäkinen K. 2019. Ribosome profiles and riboproteomes of healthy and Potato virus A- and *Agrobacterium*-infected *Nicotiana benthamiana* plants. *Mol. Plant Pathol.* 20(3):392–409
33. Lampi M, Oksanen HM, Meier F, Moldenhauer E, Poranen MM, et al. 2018. Asymmetrical flow field-flow fractionation in purification of an enveloped bacteriophage ϕ6. *J. Chromatogr. B* 1095:251–57
34. Eskelin K, Poranen MM, Oksanen HM. 2019. Asymmetrical flow field-flow fractionation on virus and virus-like particle applications. *Microorganisms* 7:555
35. Kondylis P, Schlicksup CJ, Zlotnick A, Jacobson SC. 2019. Analytical techniques to characterize the structure, properties, and assembly of virus capsids. *Anal. Chem.* 91:622–36
36. Eskelin K, Poranen MM. 2018. Controlled disassembly and purification of functional viral subassemblies using asymmetrical flow field-flow fractionation (AF4). *Viruses* 10(11):579
37. Zhang M, Yang J, Cai Z, Feng Y, Wang Y, et al. 2019. Detection of engineered nanoparticles in aquatic environments: current status and challenges in enrichment, separation, and analysis. *Environ. Sci. Nano* 6:709–35
38. Bolinsson H, Lu Y, Hall S, Nilsson L, Håkansson A. 2018. An alternative method for calibration of flow field flow fractionation channels for hydrodynamic radius determination: the nanoemulsion method (featuring multi angle light scattering). *J. Chromatogr. A* 1533:155–63
39. Mudalige TK, Qu H, Van Haute D, Ansar SM, Linder SW. 2018. Capillary electrophoresis and asymmetric flow field-flow fractionation for size-based separation of engineered metallic nanoparticles: a critical comparative review. *TrAC Trends Anal. Chem.* 106:202–12
40. Baalousha M, Stolpe B, Lead JR. 2011. Flow field-flow fractionation for the analysis and characterization of natural colloids and manufactured nanoparticles in environmental systems: a critical review. *J. Chromatogr. A* 1218(27):4078–103
41. Stone V, Nowack B, Baun A, van den Brink N, von der Kammer F, et al. 2010. Nanomaterials for environmental studies: classification, reference material issues, and strategies for physico-chemical characterisation. *Sci. Total Environ.* 408:1745–54
42. Contado C. 2015. Nanomaterials in consumer products: a challenging analytical problem. *Front. Chem.* 3:48
43. von der Kammer F, Legros S, Hofmann T, Larsen EH, Loeschner K. 2011. Separation and characterization of nanoparticles in complex food and environmental samples by field-flow fractionation. *TrAC Trends Anal. Chem.* 30:425–36
44. Pornwilard M-M, Siripinyanond A. 2014. Field-flow fractionation with inductively coupled plasma mass spectrometry: past, present, and future. *J. Anal. At. Spectrom.* 29:1739–52
45. Loosli F, Wang J, Sikder M, Afshinnia K, Baalousha M. 2020. Analysis of engineered nanomaterials (Ag, CeO_2, and Fe_2O_3) in spiked surface waters at environmentally relevant particle concentrations. *Sci. Total Environ.* 715:136927–37

46. Barber A, Kly S, Moffit MG, Rand L, Ranville JF. 2020. Coupling single particle ICP-MS with field-flow fractionation for characterizing metal nanoparticles contained in nanoplastic colloids. *Environ. Sci. Nano* 7:514–24
47. Mitrano DM, Barber A, Bednar A, Westerhoff P, Higgins CP, Ranville JF. 2012. Silver nanoparticle characterization using single particle ICP-MS (SP-ICP-MS) and asymmetrical flow field flow fractionation ICP-MS (AF4-ICP-MS). *J. Anal. At. Spectrom.* 27:1131–42
48. Yi Z, Loosli F, Wang J, Berti D, Baalousha M. 2020. How to distinguish natural versus engineered nanomaterials: insights from the analysis of TiO_2 and CeO_2 in soils. *Environ. Chem. Lett.* 18:215–27
49. Smith WC, Morse JR, Bria CRM, Schaak RE, Williams SKR. 2018. Composition-based separation of Pt-Fe_3O_4 hybrid nanoparticles by thermal field-flow fractionation. *ACS Appl. Nano Mater.* 1:6435–43
50. Dou H, Kim B-J, Choi S-H, Jung EC, Lee S. 2014. Effect of size of Fe_3O_4 magnetic nanoparticles on electrochemical performance of screen printed electrode using sedimentation field-flow fractionation. *J. Nanoparticle Res.* 16:2679–91
51. Tadjiki S, Montaño MD, Assemi S, Barber A, Ranville J, Beckett R. 2017. Measurement of the density of engineered silver nanoparticles using centrifugal FFF-TEM and single particle ICP-MS. *Anal. Chem.* 89:6056–64
52. Loosli F, Yi Z, Wang J, Baalousha M. 2019. Dispersion of natural nanomaterials in surface waters for better characterization of their physicochemical properties by AF4-ICP-MS-TEM. *Sci. Total Environ.* 682:663–72
53. López-Sanz S, Rodríguez Fariñas N, Martín-Doimeadios RCR, Ríos Á. 2019. Analytical strategy based on asymmetric flow field flow fractionation hyphenated to ICP-MS and complementary techniques to study gold nanoparticles transformations in cell culture medium. *Anal. Chim. Acta* 1053:178–85
54. Kim W, Bae J, Eum CH, Jung J, Lee S. 2018. Study on dispersibility of thermally stable carbon black particles in ink using asymmetric flow field-flow fractionation (AsFlFFF). *Microchem. J.* 142:167–74
55. Herrero P, Bäuerlein PS, Emke E, Pocurull E, de Voogt P. 2014. Asymmetrical flow field-flow fractionation hyphenated to Orbitrap high resolution mass spectrometry for the determination of (functionalised) aqueous fullerene aggregates. *J. Chromatogr. A* 1356:277–82
56. Gigault J, El Hadri H, Reynaud S, Deniau E, Grassl B. 2017. Asymmetrical flow field flow fractionation methods to characterize submicron particles: application to carbon-based aggregates and nanoplastics. *Anal. Bioanal. Chem.* 409(29):6761–69
57. Amaro-Gahete J, Benítez A, Otero R, Esquivel D, Jiménez-Sanchidrián C, et al. 2019. A comparative study of particle size distribution of graphene nanosheets synthesized by an ultrasound-assisted method. *Nanomaterials* 9:152–67
58. El Hadri H, Gigault J, Tan J, Hackley VA. 2018. An assessment of retention behavior for gold nanorods in asymmetrical flow field-flow fractionation. *Anal. Bioanal. Chem.* 410:6977–84
59. Runyon JR, Goering A, Yong KT, Williams SKR. 2013. Preparation of narrow dispersity gold nanorods by asymmetrical flow field-flow fractionation and investigation of surface plasmon resonance. *Anal. Chem.* 85:940–48
60. Chen M, Parot J, Mukherjee A, Couillard M, Zou S, et al. 2020. Characterization of size and aggregation for cellulose nanocrystal dispersions separated by asymmetrical-flow field-flow fractionation. *Cellulose* 27(4):2015–28
61. Saenmuangchin R, Siripinyanond A. 2018. Flow field-flow fractionation for hydrodynamic diameter estimation of gold nanoparticles with various types of surface coatings. *Anal. Bioanal. Chem.* 410:6845–59
62. Schwaferts C, Niessner R, Elsner M, Ivleva NP. 2019. Methods for the analysis of submicrometer- and nanoplastic particles in the environment. *TrAC Trends Anal. Chem.* 112:52–65
63. Correia M, Loeschner K. 2018. Detection of nanoplastics in food by asymmetric flow field-flow fractionation coupled to multi-angle light scattering: possibilities, challenges and analytical limitations. *Anal. Bioanal. Chem.* 410(22):5603–15
64. Qu H, Quevedo IR, Linder SW, Fong A, Mudalige TK. 2016. Importance of material matching in the calibration of asymmetric flow field-flow fractionation: material specificity and nanoparticle surface coating effects on retention time. *J. Nanoparticle Res.* 18:292–302

65. Gigault J, Hackley VA. 2013. Observation of size-independent effects in nanoparticle retention behavior during asymmetric-flow field-flow fractionation. *Anal. Bioanal. Chem.* 405(19):6251–58
66. Noskov S, Scherer C, Maskos M. 2013. Determination of Hamaker constants of polymeric nanoparticles in organic solvents by asymmetrical flow field-flow fractionation. *J. Chromatogr. A* 1274:151–58
67. Zhang X, Li Y, Shen S, Lee S, Dou H. 2018. Field-flow fractionation: a gentle separation and characterization technique in biomedicine. *TrAC Trends Anal. Chem.* 108:231–38
68. Zattoni A, Roda B, Borghi F, Marassi V, Reschiglian P. 2014. Flow field-flow fractionation for the analysis of nanoparticles used in drug delivery. *J. Pharm. Biomed. Anal.* 87:53–61
69. Wagner M, Holzschuh S, Traeger A, Fahr A, Schubert US. 2014. Asymmetric flow field-flow fractionation in the field of nanomedicine. *Anal. Chem.* 86:5201–10
70. Fan Y, Marioli M, Zhang K. 2021. Analytical characterization of liposomes and other lipid nanoparticles for drug delivery. *J. Pharm. Biomed. Anal.* 192:113642–63
71. Caputo F, Clogston J, Calzolai L, Rösslein M, Prina-Mello A. 2019. Measuring particle size distribution of nanoparticle enabled medicinal products, the joint view of EUNCL and NCI-NCL. A step by step approach combining orthogonal measurements with increasing complexity. *J. Control. Release* 299:31–43
72. Elvang PA, Stein PC, Bauer-Brandl A, Brandl M. 2017. Characterization of co-existing colloidal structures in fasted state simulated fluids FaSSIF: a comparative study using AF4/MALLS, DLS and DOSY. *J. Pharm. Biomed. Anal.* 145:531–36
73. Engel A, Plöger M, Mulac D, Langer K. 2014. Asymmetric flow field-flow fractionation (AF4) for the quantification of nanoparticle release from tablets during dissolution testing. *Int. J. Pharm.* 461:137–44
74. Contado C, Vighi E, Dalpiaz A, Leo E. 2013. Influence of secondary preparative parameters and aging effects on PLGA particle size distribution: a sedimentation field flow fractionation investigation. *Anal. Bioanal. Chem.* 405:703–11
75. Wagner M, Barthel MJ, Freund RRA, Hoeppener S, Traeger A, et al. 2014. Solution self-assembly of poly(ethylene oxide)-*block*-poly(furfuryl glycidyl ether)-*block*-poly(allyl glycidyl ether) based triblock terpolymers: a field-flow fractionation study. *Polym. Chem.* 5(24):6943–56
76. Boye S, Appelhans D, Boyko V, Zschoche S, Komber H, et al. 2012. pH-triggered aggregate shape of different generations lysine-dendronized maleimide copolymers with maltose shell. *Biomacromolecules* 13(12):4222–35
77. Pound-Lana GEN, Garcia GM, Trindade IC, Capelari-Oliveira P, Pontifice TG, et al. 2019. Phthalocyanine photosensitizer in polyethylene glycol-*block*-poly(lactide-*co*-benzyl glycidyl ether) nanocarriers: probing the contribution of aromatic donor-acceptor interactions in polymeric nanospheres. *Mater. Sci. Eng. C* 94:220–33
78. Miwa S, Takahashi R, Rössel C, Matsumoto S, Fujii S, et al. 2018. Core-shell-corona micelles from a polyether-based triblock terpolymer: investigation of the pH-dependent micellar structure. *Langmuir* 34(26):7813–20
79. Till U, Gaucher-Delmas M, Saint-Aguet P, Hamon G, Marty J-D, et al. 2014. Asymmetrical flow field-flow fractionation with multi-angle light scattering and quasi-elastic light scattering for characterization of polymersomes: comparison with classical techniques. *Anal. Bioanal. Chem.* 406(30):7841–53
80. Deodhar GV, Adams ML, Joardar S, Joglekar M, Davidson M, et al. 2018. Conserved activity of reassociated homotetrameric protein subunits released from mesoporous silica nanoparticles. *Langmuir* 34(1):228–33
81. Roda B, Marassi V, Zattoni A, Borghi F, Anand R, et al. 2018. Flow field-flow fractionation and multi-angle light scattering as a powerful tool for the characterization and stability evaluation of drug-loaded metal-organic framework nanoparticles. *Anal. Bioanal. Chem.* 410:5245–53
82. Khosa A, Reddi S, Saha RN. 2018. Nanostructured lipid carriers for site-specific drug delivery. *Biomed. Pharmacother.* 103:598–613
83. Qu H, Wang J, Wu Y, Zheng J, Krishnaiah YSR, et al. 2018. Asymmetric flow field flow fractionation for the characterization of globule size distribution in complex formulations: a cyclosporine ophthalmic emulsion case. *Int. J. Pharm.* 538:215–22

84. Elvang PA, Hinna AH, Brouwers J, Hens B, Augustijns P, Brandl M. 2016. Bile salt micelles and phospholipid vesicles present in simulated and human intestinal fluids: structural analysis by flow field-flow fractionation/multiangle laser light scattering. *J. Pharm. Sci.* 105(9):2832–39
85. Till U, Gaucher M, Amouroux B, Gineste S, Lonetti B, et al. 2017. Frit inlet field-flow fractionation techniques for the characterization of polyion complex self-assemblies. *J. Chromatogr. A* 1481:101–10
86. Parot J, Caputo F, Mehn D, Hackley VA, Calzolai L. 2020. Physical characterization of liposomal drug formulations using multi-detector asymmetrical-flow field flow fractionation. *J. Control. Release* 320:495–510
87. Hu Y, Crist RM, Clogston JD. 2020. The utility of asymmetric flow field-flow fractionation for preclinical characterization of nanomedicines. *Anal. Bioanal. Chem.* 512:425–38
88. Ashby J, Schachermeyer S, Duan Y, Jimenez LA, Zhong W. 2014. Probing and quantifying DNA-protein interactions with asymmetrical flow field-flow fractionation. *J. Chromatogr. A* 1358:217–24
89. Pollastrini J, Dillon TM, Bondarenko P, Chou RYT. 2011. Field flow fractionation for assessing neonatal Fc receptor and Fcγ receptor binding to monoclonal antibodies in solution. *Anal. Biochem.* 414:88–98
90. Bria CRM, Jones J, Charlesworth A, Williams SKR. 2016. Probing submicron aggregation kinetics of an IgG protein by asymmetrical flow field-flow fractionation. *J. Pharm. Sci.* 105(1):31–39
91. Ma D, Martin N, Tribet C, Winnik FM. 2014. Quantitative characterization by asymmetrical flow field-flow fractionation of IgG thermal aggregation with and without polymer protective agents. *Anal. Bioanal. Chem.* 406:7539–47
92. Leeman M, Choi J, Hansson S, Storm MU, Nilsson L. 2018. Proteins and antibodies in serum, plasma, and whole blood—size characterization using asymmetrical flow field-flow fractionation (AF4). *Anal. Bioanal. Chem.* 410(20):4867–73
93. Bria CRM, Williams SKR. 2016. Impact of asymmetrical flow field-flow fractionation on protein aggregates stability. *J. Chromatogr. A* 1465:155–64
94. Boll B, Josse L, Heubach A, Hochenauer S, Finkler C, et al. 2018. Impact of non-ideal analyte behavior on the separation of protein aggregates by asymmetric flow field-flow fractionation. *J. Sep. Sci.* 41(13):2854–64
95. Caracciolo G, Farokhzad OC, Mahmoudi M. 2017. Biological identity of nanoparticles in vivo: clinical implications of the protein corona. *Trends Biotechnol.* 35:257–64
96. Ojea-Jiménez I, Capomaccio R, Osório I, Mehn D, Ceccone G, et al. 2018. Rational design of multifunctional gold nanoparticles with controlled biomolecule adsorption: a multi-method approach for in-depth characterization. *Nanoscale* 10(21):10173–81
97. Safenkova IV, Slutskaya ES, Panferov VG, Zherdev AV, Dzantiev BB. 2016. Complex analysis of concentrated antibody-gold nanoparticle conjugates' mixtures using asymmetric flow field-flow fractionation. *J. Chromatogr. A* 1477:56–63
98. Bouzas-Ramos D, García-Alonso JI, Costa-Fernández JM, Ruiz Encinar J. 2019. Quantitative assessment of individual populations present in nanoparticle-antibody conjugate mixtures using AF4-ICP-MS/MS. *Anal. Chem.* 91(5):3567–74
99. Ferreira HS, Moreira-Alvarez B, Montoro Bustos AR, Encinar JR, Costa-Fernández JM, Sanz-Medel A. 2020. Capabilities of asymmetrical flow field–flow fractionation on-line coupled to different detectors for characterization of water-stabilized quantum dots bioconjugated to biomolecules. *Talanta* 206:120228–36
100. Niezabitowska E, Smith J, Prestly MR, Akhtar R, von Aulock FW, et al. 2018. Facile production of nanocomposites of carbon nanotubes and polycaprolactone with high aspect ratios with potential applications in drug delivery. *RSC Adv.* 8(30):16444–54
101. Contado C, Mehn D, Gilliland D, Calzolai L. 2019. Characterization methods for studying protein adsorption on nano-polystyrene beads. *J. Chromatogr. A* 1606:460383–94
102. Ashby J, Schachermeyer S, Pan S, Zhong W. 2013. Dissociation-based screening of nanoparticle–protein interaction via flow field-flow fractionation. *Anal. Chem.* 85:7494–7501
103. Weber C, Simon J, Mailänder V, Morsbach S, Landfester K. 2018. Preservation of the soft protein corona in distinct flow allows identification of weakly bound proteins. *Acta Biomater.* 76:217–24

104. Boye S, Ennen F, Scharfenberg L, Appelhans D, Nilsson L, Lederer A. 2015. From 1D rods to 3D networks: a biohybrid topological diversity investigated by asymmetrical flow field-flow fractionation. *Macromolecules* 48:4607–19
105. Till U, Gibot L, Mingotaud C, Vicendo P, Rols M-P, et al. 2016. Self-assembled polymeric vectors mixtures: characterization of the polymorphism and existence of synergistic effects in photodynamic therapy. *Nanotechnology* 27:315102–12
106. Fuentes C, Choi J, Zielke C, Peñarrieta JM, Lee S, Nilsson L. 2019. Comparison between conventional and frit-inlet channel in separation of biopolymers by asymmetric flow field-flow fractionation. *Analyst* 144:4559–68
107. Bria CRM, Skelly PW, Morse JR, Schaak RE, Williams SKR. 2017. Semi-preparative asymmetrical flow field-flow fractionation: a closer look at channel dimensions and separation performance. *J. Chromatogr. A* 1499:149–57
108. Marioli M, Kavurt B, Stamatialis D, Kok WT. 2019. Application of microstructured membranes for increasing retention, selectivity and resolution in asymmetrical flow field-flow fractionation. *J. Chromatogr. A* 1605:360347–56
109. Marioli M, Kok WT. 2020. Continuous asymmetrical flow field-flow fractionation for the purification of proteins and nanoparticles. *Sep. Purif. Technol.* 242:116744–53
110. Tan P, Yang J, Nischwitz V. 2020. A novel approach for determination of the dissolved and the particulate fractions in aqueous samples by flow field flow fractionation via online monitoring of both the cross flow and the detector flow using ICP-MS. *J. Anal. At. Spectrom.* 35:548–59
111. Cuss CW, Grant-Weaver I, Shotyk W. 2017. AF4-ICPMS with the 300 Da membrane to resolve metal-bearing "colloids" <1 kDa: optimization, fractogram deconvolution, and advanced quality control. *Anal. Chem.* 89:8027–35
112. Huclier-Markai S, Grivaud-Le Du A, N'tsiba E, Montavon G, Mougin-Degraef M, Barbet J. 2018. Coupling a gamma-ray detector with asymmetrical flow field flow fractionation (AF4): application to a drug-delivery system for alpha-therapy. *J. Chromatogr. A* 1573:107–14
113. Maguire CM, Rösslein M, Wick P, Prina-Mello A. 2018. Characterisation of particles in solution—a perspective on light scattering and comparative technologies. *Sci. Technol. Adv. Mater.* 19(1):732–45
114. Hu Z, Ye C, Mi W, Zhao Y, Quan C, et al. 2018. Light-scattering detection within the difficult size range of protein particle measurement using flow cytometry. *Nanoscale* 10(41):19277–85
115. Sitar S, Kejž A, Pahovnik D, Kogej K, Tuš Ek-ZM, et al. 2015. Size characterization and quantification of exosomes by asymmetrical-flow field-flow fractionation. *Anal. Chem.* 87:9225–33
116. Kato H, Nakamura A, Banno H. 2019. Determination of number-based size distribution of silica particles using centrifugal field-flow fractionation. *J. Chromatogr. A* 1602:409–18
117. Hwang JY, Youn S, Yang I-H. 2019. Gravitational field flow fractionation: enhancing the resolution power by using an acoustic force field. *Anal. Chim. Acta* 1047:238–47
118. Johann C, Elsenberg S, Schuch H, Rösch U. 2015. Instrument and method to determine the electrophoretic mobility of nanoparticles and proteins by combining electrical and flow field-flow fractionation. *Anal. Chem.* 87(8):4292–98
119. Toney M, Baiamonte L, Smith WC, Williams SKR. 2021. Field-flow fractionation techniques for polymer characterization. In *Molecular Characterization of Polymers: A Fundamental Guide*, ed. MI Malik, J Mays, MR Shah, pp. 129–71. Amsterdam: Elsevier
120. Giddings JC, Yoon YH, Myers MN. 1975. Evaluation and comparison of gel permeation chromatography and thermal field-flow fractionation for polymer separations. *Anal. Chem.* 47(1):126–31
121. Otte T, Pasch H, Macko T, Brüll R, Stadler FJ, et al. 2011. Characterization of branched ultrahigh molar mass polymers by asymmetrical flow field-flow fractionation and size exclusion chromatography. *J. Chromatogr. A* 1218(27):4257–67
122. Gunderson JJ, Giddings JC. 1986. Comparison of polymer resolution in thermal field-flow fractionation and size-exclusion chromatography. *Anal. Chim. Acta* 189:1–15
123. Meunier DM, Wade JH, Janco M, Cong R, Gao W, et al. 2021. Recent advances in separation-based techniques for synthetic polymer characterization. *Anal Chem.* 93:273–94

124. Smith WC, Geisler M, Lederer A, Williams SKR. 2019. Thermal field-flow fractionation for characterization of architecture in hyperbranched aromatic-aliphatic polyesters with controlled branching. *Anal. Chem.* 91(19):12344–51
125. Geisler M, Smith WC, Plüschke L, Mundil R, Merna J, et al. 2019. Topology analysis of chain walking polymerized polyethylene: an alternative approach for the branching characterization by thermal FFF. *Macromolecules* 52(22):8662–71
126. Viktor Z, Pasch H. 2020. Two-dimensional fractionation of complex polymers by comprehensive online-coupled thermal field-flow fractionation and size exclusion chromatography. *Anal. Chim. Acta* 1107:225–32
127. Greyling G, Pasch H. 2015. Tacticity separation of poly(methyl methacrylate) by multidetector thermal field-flow fractionation. *Anal. Chem.* 87:3011–18
128. Muza UL, Greyling G, Pasch H. 2018. Stereocomplexation of polymers in micelle nanoreactors as studied by multiple detection thermal field-flow fractionation. *Anal. Chem.* 90:13987–95
129. Muza UL, Greyling G, Pasch H. 2017. Characterization of complex polymer self-assemblies and large aggregates by multidetector thermal field-flow fractionation. *Anal. Chem.* 89:7216–24
130. Gigault J, Pettibone JM, Schmitt C, Hackley VA. 2014. Rational strategy for characterization of nanoscale particles by asymmetric-flow field flow fractionation: a tutorial. *Anal. Chim. Acta* 809:9–24
131. ISO (Int. Organ. Stand.). 2018. *ISO/TS 21362:2018 Nanotechnologies—Analysis of Nano-Objects Using Asymmetrical-Flow and Centrifugal Field-Flow Fractionation*. Geneva: ISO. **https://www.iso.org/standard/70761.html**
132. Wahlund K-G. 2013. Flow field-flow fractionation: critical overview. *J. Chromatogr. A* 1287:97–112
133. Håkansson A, Magnusson E, Bergenståhl B, Nilsson L. 2012. Hydrodynamic radius determination with asymmetrical flow field-flow fractionation using decaying cross-flows. Part I. A theoretical approach. *J. Chromatogr. A* 1253:120–26
134. Magnusson E, Håkansson A, Janiak J, Bergenståhl B, Nilsson L. 2012. Hydrodynamic radius determination with asymmetrical flow field-flow fractionation using decaying cross-flows. Part II. Experimental evaluation. *J. Chromatogr. A* 1253:127–33
135. Williams PS. 2016. Fractionating power and outlet stream polydispersity in asymmetrical flow field-flow fractionation. Part I: isocratic operation. *Anal. Bioanal. Chem.* 408(12):3247–63
136. Williams PS. 2017. Fractionating power and outlet stream polydispersity in asymmetrical flow field-flow fractionation. Part II: programmed operation. *Anal. Bioanal. Chem.* 409:317–34
137. Wang J-L, Alasonati E, Fisicaro P, Benedetti MF, Martin M. 2018. Theoretical and experimental investigation of the focusing position in asymmetrical flow field-flow fractionation (AF4). *J. Chromatogr. A* 1561:67–75
138. Dou H, Lee YJ, Jung EC, Lee BC, Lee S. 2013. Study on steric transition in asymmetrical flow field-flow fractionation and application to characterization of high-energy material. *J. Chromatogr. A* 1304:211–19
139. Dou H, Jung EC, Lee S. 2015. Factors affecting measurement of channel thickness in asymmetrical flow field-flow fractionation. *J. Chromatogr. A* 1393:115–21
140. Mudalige TK, Qu H, Linder SW. 2017. Rejection of commonly used electrolytes in asymmetric flow field flow fractionation: effects of membrane molecular weight cutoff size, fluid dynamics, and valence of electrolytes. *Langmuir* 33(6):1442–50
141. Jochem A-R, Ankah GN, Meyer L-A, Elsenberg S, Johann C, Kraus T. 2016. Colloidal mechanism of gold mechanisms of gold nanoparticle loss in asymmetric flow field-flow fractionation. *Anal. Chem.* 88(20):10065–73
142. Williams SKR, Caldwell KD. 2012. *Field-Flow Fractionation in Biopolymer Analysis*. Wien: Springer-Verlag
143. Kato H, Nakamura A, Banno H, Shimizu M. 2018. Separation of different-sized silica nanoparticles using asymmetric flow field-flow fractionation by control of the Debye length of the particles with the addition of electrolyte molecules. *Colloids Surfaces A* 538:678–85
144. Geisler M, Lederer A. 2020. Non-parabolicity correction for fifty-nine solvents and a retention study for strongly distorted flow-profiles in thermal field-flow fractionation. *J. Chromatogr. A* 1621:461082–90

145. Sitar S, Vezočnik V, Maček P, Kogej K, Pahovnik D, Žagar E. 2017. Pitfalls in size characterization of soft particles by dynamic light scattering online coupled to asymmetrical flow field-flow fractionation. *Anal. Chem.* 89(21):11744–52
146. Wyatt PJ. 2014. Measurement of special nanoparticle structures by light scattering. *Anal. Chem.* 86(15):7171–83
147. Zielke C, Fuentes C, Piculell L, Nilsson L. 2018. Co-elution phenomena in polymer mixtures studied by asymmetric flow field-flow fractionation. *J. Chromatogr. A* 1532:251–56
148. Perez-Rea D, Zielke C, Nilsson L. 2017. Co-elution effects can influence molar mass determination of large macromolecules with asymmetric flow field-flow fractionation coupled to multiangle light scattering. *J. Chromatogr. A* 1506:138–41

Annual Review of Analytical Chemistry

Volume 14, 2021

Contents

AI in Measurement Science
Chao Liu and Jiashu Sun 1

Recent Progress in the Analytical Chemistry of Champagne and Sparkling Wines
Gérard Liger-Belair and Clara Cilindre 21

3D Printed Electrochemical Sensors
Aya Abdalla and Bhavik Anil Patel 47

Bipolar (Bio)electroanalysis
Laurent Bouffier, Dodzi Zigah, Neso Sojic, and Alexander Kuhn 65

In Situ X-Ray Techniques for Electrochemical Interfaces
Bruna F. Baggio and Yvonne Grunder 87

Electrochemical Affinity Assays/Sensors: Brief History and Current Status
Kenneth R. Wehmeyer, Ryan J. White, Peter T. Kissinger, and William R. Heineman 109

Active Flow Control and Dynamic Analysis in Droplet Microfluidics
Nan Shi, Md Mohibullah, and Christopher J. Easley 133

Environmental Toxicology Assays Using Organ-on-Chip
Patarajarin Akarapipad, Kattika Kaarj, Yan Liang, and Jeong-Yeol Yoon 155

Recent Advances in Microfluidically Spun Microfibers for Tissue Engineering and Drug Delivery Applications
Joseph Scott Magnani, Reza Montazami, and Nicole N. Hashemi 185

Analytical Technologies for Liquid Biopsy of Subcellular Materials
Camila D.M. Campos, Katie Childers, Sachindra S.T. Gamage, Harshani Wijerathne, Zheng Zhao, and Steven A. Soper 207

Aqueous Two-Phase Systems and Microfluidics for Microscale Assays and Analytical Measurements
Tasdiq Ahmed, Cameron Yamanishi, Taisuke Kojima, and Shuichi Takayama 231

New Advances and Applications in Field-Flow Fractionation
Christine L. Plavchak, William C. Smith, Carmen R.M. Bria, and S. Kim Ratanathanawongs Williams 257

Biochemical Sensing with Nanoplasmonic Architectures: We Know How but Do We Know Why?
Andreas Dahlin 281

Protein Dynamics by Two-Dimensional Infrared Spectroscopy
Goran W. Tumbic, Md Yeathad Hossan, and Megan C. Thielges 299

The Role of Raman Spectroscopy Within Quantitative Metabolomics
Cassio Lima, Howbeer Muhamadali, and Royston Goodacre 323

Noncontact Nanoscale Imaging of Cells
David Klenerman, Yuri Korchev, Pavel Novak, and Andrew Shevchuk 347

Glycan Labeling and Analysis in Cells and In Vivo
Bo Cheng, Qi Tang, Che Zhang, and Xing Chen 363

Developments and Ongoing Challenges for Analysis of Surface-Bound Proteins
Tobias Weidner and David G. Castner 389

Real-Time Visualization and Monitoring of Physiological Dynamics by Aggregation-Induced Emission Luminogens (AIEgens)
Xuewen He, Jacky W.Y. Lam, Ryan T.K. Kwok, and Ben Zhong Tang 413

Clinical Chemistry for Developing Countries: Mass Spectrometry
Suji Lee, Kavyasree Chintalapudi, and Abraham K. Badu-Tawiah 437

Current Challenges and Recent Developments in Mass Spectrometry–Based Metabolomics
Stephanie L. Collins, Imhoi Koo, Jeffrey M. Peters, Philip B. Smith, and Andrew D. Patterson 467

Environmental Aspects of Oxide Nanoparticles: Probing Oxide Nanoparticle Surface Processes Under Different Environmental Conditions
Izaac Sit, Haibin Wu, and Vicki H. Grassian 489

Errata

An online log of corrections to *Annual Review of Analytical Chemistry* articles may be found at http://www.annualreviews.org/errata/anchem